

1 **Full Title:**

2 AICAR induces apoptosis and inhibits migration of prostate cancer cells through an
3 AMPK/mTOR-dependent pathway

4

5 **Running Title:**

6 AICAR inhibits the growth of prostate cancer cells through an
7 AMPK/mTOR-dependent pathway

8

9 **Authors and affiliations:**

10 Chia-Cheng Su^{1,2,3,#}, Kun-Lin Hsieh^{1,#}, Shu-Chi Wang⁴, Hsin-Chih Yeh^{5,6}, Shu-Pin
11 Huang⁵, Po-Len Liu⁷, Shih-Hua Fang⁸, Wei-Chung Cheng⁹, Kuan-Hua Huang¹,
12 Fang-Yen Chiu², I-Ling Lin⁴, Ming-Yii Huang^{10,11,*}, Chia-Yang Li^{2,*}

13

14 ¹ Division of Urology, Department of Surgery, Chi-Mei Medical Center, Tainan
15 71004, Taiwan.

16 ² Graduate Institute of Medicine, College of Medicine, Kaohsiung Medical University,
17 Kaohsiung 80708, Taiwan.

18 ³ Department of Senior Citizen Service Management, Chia Nan University of
19 Pharmacy and Science, Tainan 71710, Taiwan.

20 ⁴ Department of Medical Laboratory Science and Biotechnology, College of Health

21 Sciences, Kaohsiung Medical University, Kaohsiung 80708, Taiwan.

22 ⁵ Department of Urology, Kaohsiung Medical University Hospital and Department of

23 Urology, School of Medicine, College of Medicine, Kaohsiung Medical University,

24 Kaohsiung 80708, Taiwan.

25 ⁶ Department of Urology, Kaohsiung Municipal Ta-Tung Hospital, Kaohsiung 80145,

26 Taiwan.

27 ⁷ Department of Respiratory Therapy, College of Medicine, Kaohsiung Medical

28 University, Kaohsiung 80708, Taiwan.

29 ⁸ Institute of Athletics, National Taiwan University of Sport, Taichung 40404,

30 Taiwan.

31 ⁹ Graduate Institute of Biomedical Sciences, and Research Center for Tumor Medical

32 Science, and Drug development center, China Medical University, Taichung 40402,

33 Taiwan.

34 ¹⁰ Department of Radiation Oncology, Kaohsiung Medical University Hospital,

35 Kaohsiung 80756, Taiwan

36 ¹¹ Department of Radiation Oncology, College of Medicine, and Center for

37 Biomarkers and Biotech Drugs, Kaohsiung Medical University, Kaohsiung 80708,

38 Taiwan

39 #These authors contributed equally to this work.

40 *Correspondence and requests for materials should be addressed to M.-Y. H.

41 (miyihu@gmail.com) or C.-Y.L. (email: chiayangli@kmu.edu.tw)

42

43 CS: s2341438@yahoo.com.tw

44 KH: samlin.hsieh@gmail.com

45 SW: shuchiwang@kmu.edu.tw

46 HY: patrick1201.tw@yahoo.com.tw

47 SH: shpihu73@gmail.com

48 PL: kisa@kmu.edu.tw

49 SF: shfang@ntupes.edu.tw

50 WC: cwc0702@gmail.com

51 KH: skhsteven@gmail.com

52 FC: fangyen0210@hotmail.com

53 IL: linili@kmu.edu.tw

54 MH: miyihu@gmail.com

55 CL: chiayangli@kmu.edu.tw

56

57

58

59 **Abstract**

60 AICAR (5-aminoimidazole-4-carbox-amide-1- β -D-ribofuranoside), an
61 AMP-activated protein kinase (AMPK) agonist, has demonstrated antitumor activities
62 for several types of cancers. However, the activity of AICAR on the cell growth and
63 metastasis of prostate cancer has not been extensively studied. Herein we examine the
64 effects of AICAR on the cell growth and metastasis of prostate cancer cells, 22RV1
65 cells. Cell growth was performed by MTT assay and soft agar assay. Cell apoptosis
66 was examined by Annexin V/PI staining and PARP cleavage Western blot. Cell
67 migration was evaluated by wound-healing assay. The expression of EMT-related
68 protein and the activity of the AMPK/ mTOR-dependent pathway were analyzed by
69 Western blot. In addition, we also tested the effect of AICAR on the chemosensitivity
70 to docetaxel using MTT assay. Our results indicated that AICAR inhibits cell growth,
71 induces apoptosis, attenuates TGF- β -induced cell migration and EMT-related protein
72 expression, and enhances the chemosensitivity to docetaxel through regulating the
73 AMPK/mTOR-dependent pathway. Collectively, these findings support AICAR as a
74 potential therapeutic agent for the treatment of prostate cancer.

75

76 Keywords: AICAR, AMPK, Prostate cancer, Metastasis, Chemosensitivity

77

78 **Introduction**

79 Prostate cancer is the most common cancer and the second leading cause of
80 cancer-related death among men in the United States [1]. Current treatment options
81 for prostate cancer include surgery, hormonal therapy, chemotherapy, radiation
82 therapy, radiofrequency ablation, high-intensity focused ultrasound, cryotherapy, and
83 cancer vaccine [2, 3]. Androgen deprivation therapy (ADT) by surgical or chemical
84 castration has been the mainstay of treatment for advanced prostate cancer in the past
85 few decades. However, the majority of androgen-sensitive prostate cancer patients
86 will eventually develop resistance to ADT within 1 to 3 years and the disease will
87 become androgen-independent [4]. Currently, there is no effective therapy for
88 recurrent prostate cancer. Hence, a novel therapeutic method for prostate cancer is
89 needed.

90 The 5'-adenosine monophosphate (AMP)-activated protein kinase (AMPK) is
91 activated by increases in cellular ATP/AMP ratio and plays an important role in
92 regulating glycolytic activity and maintaining energy balance at both cellular and
93 whole body levels [5]. Previous studies indicated that AMPK exhibits intricate
94 relations with other energy/metabolite sensor pathways (e.g. SIRT1, Akt, mTOR,
95 PARPs, etc.) and acts in a coordinated fashion with these [6-10]. AMPK induction

96 leads to enhanced mitochondrial oxidation and mitochondrial biogenesis that have
97 been shown to exert anti-Warburg and anti-proliferative effects in several types of
98 cancers, such as leukemia [11], breast cancer [12], pancreatic cancer [13],
99 hepatocellular carcinoma [14], and prostate cancer [15]. These findings suggest that
100 AMPK activation may be used beneficially for cancer treatment.

101 The adenoside analog compound,
102 5-aminoimidazole-4-carbox-amide-1- β -D-ribofuranoside (AICAR), is intracellularly
103 converted by adenosine kinase to the non-phosphorylated derivative
104 amino-imidazolecarboxamide ribonucleotide (ZMP), an analogue of AMP, which
105 activates AMPK [16]. Therefore, AICAR is often used as an activator of AMPK [17]
106 to modulate cellular energy homeostasis, although AMPK-independent effects have
107 also been proposed [18, 19]. A previous study indicated that AICAR inhibited the
108 growth of androgen-independent (DU145, PC3) and androgen-sensitive (LNCaP)
109 cells after four days of treatment [20]. In addition, AICAR inhibited two key enzymes
110 involved in protein synthesis, mTOR and p70S6K, and blocked the ability of the
111 androgen R1881 to increase cell growth and the expression of two enzymes for *de*
112 *novo* fatty acid synthesis, acetyl CoA carboxylase and fatty acid synthase, in the
113 LNCaP cells [20]. A current study showed that AICAR induced AMPK-independent
114 programmed necrosis in prostate cancer cells [21]. Collectively, these studies indicate

115 that AICAR has potential in inhibiting the growth of prostate cancer. However, the
116 effect of AICAR on the apoptosis and migration of prostate cancer remains unclear. In
117 the present study, we evaluated the effects of AICAR on apoptotic activity, migration
118 and chemosensitivity through AMPK phosphorylation in human prostate cancer cells.

119

120

121

122

123

124

125

126

127

128

129

130

131

132

133

134

135 **Materials and Methods**

136 **Reagents**

137 RPMI 1640 medium, penicillin, streptomycin and fetal bovine serum (FBS) were
138 purchased from Gibco-BRL (Life Technologies, Grand Island, NY, USA). AICAR,
139 bovine serum albumin (BSA), phosphate-buffered saline (PBS), RIPA buffer,
140 protease inhibitor cocktail, phosphatase inhibitor cocktail, stripping buffer,
141 thioglycollate medium, and 3-(4,5-dimethylthiazol-2-yl)-2, 5-diphenyl tetrazolium
142 bromide (MTT) were purchased from Sigma Aldrich (St. Louis, MO, USA). AICAR
143 was purchased from Cayman Chemical (Ann Arbor, MI, USA). Alexa Fluor® 488
144 Annexin V/Dead Cell Apoptosis Kit was purchased from Thermo Fisher Scientific
145 (Eugene, Oregon, OR, USA). BCA protein assay reagent was purchased from Thermo
146 Scientific (Waltham, MA, USA). For western blotting, rabbit antibodies against
147 human phospho-AMPK, AMPK, MYC, mTOR, PARP, phospho-p70S6K, p70S6K,
148 TSC-1, TSC-2, β -actin and secondary antibodies were purchased from Cell Signaling
149 (Farmingdale, NY, USA). Caspase-Glo 3/7 assay kit was purchased from Promega
150 (Madison, WI, USA). Transforming growth factor-beta 1 was purchased from
151 PeproTech (Rocky Hill, NJ, USA). Docetaxel (Taxothere, 20 mg/mL) was obtained
152 from Sanofi Aventis (Germany).

153

154 **Cell culture**

155 Human prostate cancer cell line, 22Rv1, purchased from Bioresource Collection and
156 Research Center (Food Industry Research and Development Institute, Hsinchu,
157 Taiwan), and was cultured in RPMI 1640 supplemented with antibiotics (100 U/mL
158 penicillin and 100 U/mL streptomycin) and 10% (v/v) FBS in a humidified
159 atmosphere of 5% CO₂ at 37°C and passaged every 2-3 days to maintain growth.

160

161 **MTT assay**

162 22Rv1 cells were seeded in a 96-well plate at a concentration of 1×10^5 cells, and
163 were allowed to acclimatize overnight. Cells were treated with various concentrations
164 of the AICAR (0, 0.5, 1 and 3 mM) for 24 hr. Cell viability was measured by the
165 ability of viable cells to reduce MTT to formazan based on the ability of living cells
166 utilized thiazolyl blue and converted it into purple formazan. The concentration of
167 formazan is measured by determining the OD at 570 nm using a microplate reader
168 (BioTek Instruments, Inc., Winooski, VT, USA). The results are given as relative
169 percentage to the untreated control. To detect the synergistic effects of AICAR, cells
170 were treated with different doses of the AICAR (0, 0.5, and 1 mM) combined with
171 different doses of docetaxel for 24 and 48 hr.

172

173 **Soft agar colony formation assay**

174 Noble agar (BD Biosciences, Franklin Lakes, NJ, USA) was dissolved in complete
175 medium and coated with 0.5% agar solution on the bottom of 6-well plates. After
176 solidifying, top agar medium mixture (0.3%) containing 5×10^3 cells was added, and
177 incubated at 37 °C in a humidified atmosphere of 5% CO₂ for 3 weeks. Colonies were
178 stained with 0.05% crystal violet-10% ethanol in PBS. Photographs of the
179 stained colonies were captured using Bio-Rad ChemiDoc XRS⁺ system (Bio-Rad
180 Laboratories, Inc., Hercules, CA, USA) and quantified using ImageJ software
181 (National Institutes of Health, Bethesda, MD, USA).

182

183 **Apoptosis assay**

184 22Rv1 cells were treated with different doses of AICAR (0, 0.5, 1, and 3 mM) for 24
185 hr. Cells were trypsinized, washed twice by cold PBS, and stained with Alexa Fluor®
186 488 Annexin V and propidium iodide (PI) according to manufacturer's protocol
187 (Thermo Fisher Scientific, Rockford, IL, USA). Apoptotic cells were determined
188 using FC500 flow cytometer (Beckman-Coulter, Fullerton, CA, USA). Ten thousand
189 events were collected per sample. Data were analyzed by CXP analysis software
190 (Beckman-Coulter, Fullerton, CA, USA).

191

192 **Western blot**

193 Cells were lysed by RIPA buffer with protease inhibitors and phosphatase inhibitors
194 according to the manufacturer's protocol (Sigma Aldrich, St. Louis, MO, USA). The
195 protein concentration was determined using the BCA protein assay reagent according
196 to the manufacturer's instructions (Thermo Scientific, Waltham, MA, USA). Cellular
197 protein extracts were separated by electrophoresis using 8% SDS polyacrylamide gel
198 and were electroblotted onto PVDF membranes. The membranes were incubated with
199 blocking solution for 1 hr at room temperature, followed by incubation overnight with
200 primary antibodies at 4 °C (1:1000). Blots were washed three times with Tris-buffered
201 saline/Tween 20 (TBST) and incubated with a 1:5000 dilution of horseradish
202 peroxidase conjugated secondary antibody for 1 hr at room temperature. Blots were
203 again washed three times with TBST and developed using an ECL
204 chemiluminescence substrate (Thermo Scientific, Waltham, MA, USA). The signals
205 were captured and the band intensities were quantified using Bio-Rad ChemiDoc
206 XRS⁺ system (Bio-Rad Laboratories, Inc., Hercules, CA, USA).

207

208 **Caspase 3/7 activity assay**

209 22Rv1 cells were seeded in a 96-well white plate at a concentration of 2.5×10^4 cells,

210 and were allowed to acclimatize overnight. Cells were treated with various
211 concentrations of the AICAR (0, 0.5, 1, and 3 mM) for 24 hr. A total of 100 μ L
212 Caspase-Glo[®] 3/7 reagent was added to each well, gently mixed contents of wells
213 using a plate shaker at 300~500 rpm for 30 seconds, and then samples were incubated
214 for 30 min at RT. Enzyme activity is directly proportional to luminescence, which
215 was measured using a luminescence microplate reader (BioTek Instruments, Inc.,
216 Winooski, VT, USA). Data were normalized relative to the caspase 3/7 activity of
217 cells treated with DMSO alone.

218

219 **Migration assay**

220 SPLScar[™] Block (SPL life sciences, Korea) was placed in a 24-well plate, seeded 5 x
221 10⁴ cells in each side of block, and was allowed to acclimatize overnight. The block
222 was removed, replaced flash medium, and treated cells with 5 ng/ml TGF- β 1 and
223 different concentrations of AICAR. Cell migration was monitored under a
224 phase-contrast microscope and the migratory distance was calculated.

225

226 **Statistical analysis**

227 All data are expressed as means \pm SD. Each value is the mean of three independent
228 experiments. Statistical analysis was assessed via Student's *t*-test using IBM SPSS

229 Statistics v.19 (IBM Corp., Armonk, NY, USA), and the significant difference was set

230 at $*p < 0.05$; $**p < 0.01$; $***p < 0.001$.

231

232

233

234

235

236

237

238

239

240

241

242

243

244

245

246

247

248

249 **Results**

250 **AICAR inhibits the growth of prostate cancer cells**

251 The 22Rv1 cell line is an androgen-independent prostate cancer epithelial cell line
252 that is representative of clinical recurrent prostate cancer [22]. Firstly, we examined
253 the effect of AICAR on the growth of 22Rv1 prostate cancer cells. Cells were treated
254 with various concentrations (0, 0.5, 1 and 3 mM) of AICAR for 24 hr. Cell viability
255 was analyzed by MTT assay. The experimental results showed that AICAR inhibits
256 the growth of 22Rv1 cells in a dose-dependent manner (Fig. 1A). In addition, we
257 further examined whether AICAR affects the colony growth under
258 anchorage-independent condition. Cells were treated with different concentrations (0,
259 0.25, 0.5 and 1 mM) of AICAR and then conducted a soft agar assay. The
260 experimental results showed that AICAR suppressed growth of 22Rv1 cells in soft
261 agar in a dose-dependent manner (Fig. 1B).

262

263 **AICAR induces apoptosis in prostate cancer cells**

264 To further test whether AICAR induces apoptosis in prostate cancer cells, 22Rv1 cells
265 were treated with various concentrations (0, 0.5, 1 and 3 mM) of AICAR for 24 hr.
266 Apoptotic cells were detected with Annexin V/PI staining using flow cytometry. Our

267 results demonstrated that AICAR induced apoptosis (Fig. 2A). Poly(ADP-ribose)
268 polymerase (PARP) is a nuclear enzyme involved in DNA repair which is cleaved by
269 caspase-3 during apoptosis [23]. We further examined whether AICAR affects the
270 expression of PARP in 22Rv1 cells. As shown in Figure 2B, AICAR increased the
271 expression of cleaved PARP, an apoptosis marker, in 22Rv1 cells. In addition, we
272 also examined the activity of caspase 3/7 using a luminescent substrate based assay.
273 Our results indicated that AICAR increased the activity of caspase 3/7 in 22Rv1 cells
274 (Fig. 2C).

275

276 **AICAR inhibits transforming growth factor-beta (TGF- β)-induced migration**
277 **and epithelial to mesenchymal transition (EMT)**

278 TGF- β signaling is well known as a key regulator of many biological processes in
279 prostate cancer including inducing EMT, migration and metastasis [24]. To examine
280 whether AICAR affects TGF- β -induced migration and EMT in prostate cancer cells,
281 22Rv1 cells were treated with 5 ng/mL TGF- β and various concentrations (0, 0.25 and
282 0.5 mM) of AICAR. Cell migration was performed by counting the average wound
283 space. Our results showed that AICAR significantly inhibited TGF- β -induced
284 migration (Fig. 3A and 3B). In addition, we also analyzed the expression of
285 EMT-related proteins using Western blot. As shown in Figure 3C, AICAR inhibited

286 TGF- β -induced EMT through inhibiting the expression of mesenchymal marker,
287 N-cadherin, and enhancing the expression of epithelial marker, E-cadherin.

288

289 **AICAR exhibits synergistic effect with docetaxel treatment**

290 Docetaxel-based therapy has been applied as the first-line chemotherapy for
291 metastatic castration-resistant prostate cancer (mCRPC) for a decade due to its ability
292 to improve the median overall survival (OS) by around 3 months [25, 26]. To examine
293 whether AICAR affects the therapeutic efficiency of docetaxel-based therapy in
294 prostate cancer, 22Rv1 cells were treated with various doses (0, 0.5 and 1 mM) of
295 AICAR in the presence or absence of docetaxel for 24 hr. Cell survival was analyzed
296 by MTT assay. As shown in Fig. 4, AICAR exhibited synergistic effect with
297 docetaxel treatment in prostate cancer cells.

298

299 **AICAR inhibits the growth of prostate cancer cells through activating an** 300 **AMPK/mTOR-dependent pathway**

301 AMPK is an upstream regulator in modulating the activation of TSC1 and TSC2
302 which consequently inhibits cell survival and proliferation via repressed
303 mTOR-p70S6K-MYC signaling pathway [27, 28]. To investigate the mechanism of
304 action of AICAR in regulating the activity of AMPK-dependent pathway, 22Rv1 cells

305 were treated with different concentrations (0, 0.5, 1 and 3 mM) of AICAR. The
306 expression of phospho-AMPK, AMPK, TSC-1, TSC-2, mTOR, phospho-p70S6K,
307 p70S6K and MYC was analyzed by Western blot. As shown in Fig. 5A, AICAR
308 promoted the phosphorylation of AMPK in 22Rv1 cells. In addition, our experimental
309 results showed that AICAR enhanced the expression of TSC1 and TSC2 (Fig. 5B),
310 whereas AICAR reduced the expression of mTOR and MYC as well as decreased the
311 phosphorylation of p70S6K (Fig. 5C). These results suggest that AICAR inhibits the
312 growth of prostate cancer cells through an AMPK/mTOR-dependent pathway (Fig.
313 5D).

314

315

316

317

318

319

320

321

322

323

324

325 **Discussion**

326 AMPK is an important regulator of cellular energy homeostasis [29]. Several agents
327 have been demonstrated to activate AMPK, including metformin and phenformin,
328 which increase the AMP:ATP ratio, the nucleoside AICAR which is metabolized to
329 an AMP mimetic, and A769662, which is a direct activator of AMPK [30]. Although
330 a number of studies indicated an anti-cancer role for AMPK [9, 11, 12, 14, 15, 31],
331 the effect of an AMPK activator, AICAR, in regulating the pathological processes of
332 prostate cancer remains enigmatic. Previous studies have shown that AICAR could
333 exert cytotoxic effect on cancer cells via AMPK-dependent and/or
334 AMPK-independent mechanisms [16, 31-33]. However, the cytotoxic effect on
335 prostate cancer remains controversial. Guo et al. indicated that AICAR induces
336 programmed necrosis, but not apoptosis, in prostate cancer cells, LNCaP, PC-3 and
337 PC-82 cells through AMPK-independent pathways [21]. In contrast, Sauer et al.
338 demonstrated that AICAR induces apoptosis of DU-145 prostate cancer cells through
339 the AMPK/mTOR-dependent signaling pathway [16]. Our experimental results
340 indicated that AICAR induces apoptosis, but not necrosis, in 22Rv1 prostate cancer
341 cells. These results point out that AICAR inhibits cell growth and induces cell death
342 in different prostate cancer cell lines probably through different mechanisms. In

343 addition, AMPK is an upstream regulator in modulating the activation of TSC1 and
344 TSC2, which consequently inhibits cell survival and proliferation via repressed
345 mTOR-p70S6K-MYC signaling pathway [27, 28]. Our experimental results showed
346 that AICAR enhances the expression of TSC1 and TSC2, whereas it reduces the
347 expression of mTOR and MYC as well as decreases the phosphorylation of p70S6K
348 in 22Rv1 prostate cancer cells. We suggest that AICAR induces apoptosis and inhibits
349 migration of prostate cancer cells through an AMPK/mTOR-dependent pathway.

350 Cancer metastasis is the major cause of morbidity and mortality; approximately
351 80% of the men who have expired from prostate cancer possessed bone metastases
352 [34]. Our experimental results indicated that AICAR suppresses TGF- β -induced cell
353 migration and inhibits TGF- β -induced EMT by decreasing the expression of a
354 mesenchymal-related marker, N-cadherin and enhancing the expression of an
355 epithelial-related marker, E-cadherin in 22Rv1 prostate cancer cells. A recent study
356 also indicated that treatment of AICAR suppresses migration and invasion in PC3 and
357 PC3M prostate cancer cells [15]. These results implied that AICAR might have
358 potential in inhibiting the metastatic activity in prostate cancer.

359 Docetaxel is a first-line treatment for CRPC, which confers survival advantages
360 of approximately 2 months for patients with low overall survival benefit [35].
361 However, treatment with docetaxel usually causes adverse side effects including hair

362 loss, myelosuppression, neurotoxicity, diarrhea etc. Our experimental results showed
363 that AICAR has synergistic effect with docetaxel treatment. These results suggest that
364 AICAR increases the sensitization of prostate cancer cells to docetaxel-induced
365 apoptosis, which might have benefit for reducing toxicity of chemotherapy in prostate
366 cancer patients.

367 In summary, our experimental results indicated that AICAR inhibits cell growth,
368 induces apoptosis, attenuates cell migration, enhances chemosensitivity to docetaxel,
369 and suppresses the activation of the AMPK/mTOR-dependent signaling pathway.
370 These results suggest that AICAR appears as a new potential anticancer agent for
371 treating prostate cancer.

372

373

374

375

376

377

378

379

380

381

382 **Funding:**

383 This study was supported by Kaohsiung Medical University (Grant No.
384 KMU-M106023), Kaohsiung Medical University Hospital (Grant No.
385 KMUH107-7R73), China Medical University (Grant No. CMU106-N-05), and
386 Chi-Mei Medical Center, Liouying (CLFHR10613). This study also supported by the
387 Ministry of Science and Technology, Taiwan, R.O.C. (Grant No. MOST
388 106-2221-E-039-011-MY3, MOST 107-2320-B-037-019 and MOST
389 107-2314-B-037-047).

390

391 **Competing interests:**

392 The authors declare that they have no conflict of interest.

393

394 **Author Contributions:**

395 **Conceptualization:** CS SF WC MH CL.

396 **Data curation:**CS KLH SW HY SH PL KHH FC IL.

397 **Formal analysis:** CS KLH SW FC.

398 **Funding acquisition:** KLH WC MH CL.

399 **Investigation:** CS KLH MH CL.

400 **Methodology:** SH MH CL.

401 **Project administration:** MH CL.

402 **Resources:** MH CL.

403 **Supervision:** MH CL.

404 **Validation:** CS KLH FC.

405 **Visualization:** CS KLH MH CL.

406 **Writing – original draft:** CS CL.

407 **Writing – review & editing:** HY SF SH MH CL

408

409

410

411

412

413

414

415

416

417

418

419

420 **Reference**

- 421 1. Siegel RL, Miller KD, Jemal A. Cancer statistics, 2018. *CA Cancer J Clin.*
422 2018;68(1):7-30. doi: 10.3322/caac.21442. PubMed PMID: 29313949.
- 423 2. Litwin MS, Tan HJ. The Diagnosis and Treatment of Prostate Cancer: A Review.
424 *JAMA.* 2017;317(24):2532-42. doi: 10.1001/jama.2017.7248. PubMed PMID:
425 28655021.
- 426 3. Marshall S, Taneja S. Focal therapy for prostate cancer: The current status.
427 *Prostate Int.* 2015;3(2):35-41. doi: 10.1016/j.pnil.2015.03.007. PubMed PMID:
428 26157765; PubMed Central PMCID: PMC4494637.
- 429 4. Asmane I, Ceraline J, Duclos B, Rob L, Litique V, Barthelemy P, et al. New
430 strategies for medical management of castration-resistant prostate cancer.
431 *Oncology.* 2011;80(1-2):1-11. doi: 10.1159/000323495. PubMed PMID:
432 21577012.
- 433 5. Grahame Hardie D. Regulation of AMP-activated protein kinase by natural and
434 synthetic activators. *Acta Pharm Sin B.* 2016;6(1):1-19. doi:
435 10.1016/j.apsb.2015.06.002. PubMed PMID: 26904394; PubMed Central PMCID:
436 PMC4724661.
- 437 6. Bai P, Nagy L, Fodor T, Liaudet L, Pacher P. Poly(ADP-ribose) polymerases as

- 438 modulators of mitochondrial activity. *Trends Endocrinol Metab.*
439 2015;26(2):75-83. doi: 10.1016/j.tem.2014.11.003. PubMed PMID: 25497347.
- 440 7. Hardie DG. AMP-activated/SNF1 protein kinases: conserved guardians of
441 cellular energy. *Nat Rev Mol Cell Biol.* 2007;8(10):774-85. doi:
442 10.1038/nrm2249. PubMed PMID: 17712357.
- 443 8. Hsu PP, Sabatini DM. Cancer cell metabolism: Warburg and beyond. *Cell.*
444 2008;134(5):703-7. doi: 10.1016/j.cell.2008.08.021. PubMed PMID: 18775299.
- 445 9. Icard P, Lincet H. A global view of the biochemical pathways involved in the
446 regulation of the metabolism of cancer cells. *Biochim Biophys Acta.*
447 2012;1826(2):423-33. doi: 10.1016/j.bbcan.2012.07.001. PubMed PMID:
448 22841746.
- 449 10. Kroemer G. Mitochondria in cancer. *Oncogene.* 2006;25(34):4630-2. doi:
450 10.1038/sj.onc.1209589. PubMed PMID: 16892077.
- 451 11. Kishton RJ, Barnes CE, Nichols AG, Cohen S, Gerriets VA, Siska PJ, et al.
452 AMPK Is Essential to Balance Glycolysis and Mitochondrial Metabolism to
453 Control T-ALL Cell Stress and Survival. *Cell Metab.* 2016;23(4):649-62. doi:
454 10.1016/j.cmet.2016.03.008. PubMed PMID: 27076078; PubMed Central
455 PMCID: PMC4832577.
- 456 12. Fodor T, Szanto M, Abdul-Rahman O, Nagy L, Der A, Kiss B, et al. Combined

- 457 Treatment of MCF-7 Cells with AICAR and Methotrexate, Arrests Cell Cycle
458 and Reverses Warburg Metabolism through AMP-Activated Protein Kinase
459 (AMPK) and FOXO1. PLoS One. 2016;11(2):e0150232. doi:
460 10.1371/journal.pone.0150232. PubMed PMID: 26919657; PubMed Central
461 PMCID: PMC4769015.
- 462 13. Cheng X, Kim JY, Ghafoory S, Duvaci T, Rafiee R, Theobald J, et al.
463 Methylisoidigo preferentially kills cancer stem cells by interfering cell
464 metabolism via inhibition of LKB1 and activation of AMPK in PDACs. Mol
465 Oncol. 2016. doi: 10.1016/j.molonc.2016.01.008. PubMed PMID: 26887594.
- 466 14. Park SY, Lee YK, Kim HJ, Park OJ, Kim YM. AMPK interacts with beta-catenin
467 in the regulation of hepatocellular carcinoma cell proliferation and survival with
468 selenium treatment. Oncol Rep. 2016;35(3):1566-72. doi: 10.3892/or.2015.4519.
469 PubMed PMID: 26707164.
- 470 15. Choudhury Y, Yang Z, Ahmad I, Nixon C, Salt IP, Leung HY. AMP-activated
471 protein kinase (AMPK) as a potential therapeutic target independent of PI3K/Akt
472 signaling in prostate cancer. Oncoscience. 2014;1(6):446-56. PubMed PMID:
473 25594043; PubMed Central PMCID: PMC4284621.
- 474 16. Sauer H, Engel S, Milosevic N, Sharifpanah F, Wartenberg M. Activation of
475 AMP-kinase by AICAR induces apoptosis of DU-145 prostate cancer cells

- 476 through generation of reactive oxygen species and activation of c-Jun N-terminal
477 kinase. *Int J Oncol.* 2012;40(2):501-8. doi: 10.3892/ijo.2011.1230. PubMed
478 PMID: 22002081.
- 479 17. Fogarty S, Hardie DG. Development of protein kinase activators: AMPK as a
480 target in metabolic disorders and cancer. *Biochim Biophys Acta.*
481 2010;1804(3):581-91. doi: 10.1016/j.bbapap.2009.09.012. PubMed PMID:
482 19778642.
- 483 18. Jacobs RL, Lingrell S, Dyck JR, Vance DE. Inhibition of hepatic
484 phosphatidylcholine synthesis by 5-aminoimidazole-4-carboxamide-1-
485 beta-4-ribofuranoside is independent of AMP-activated protein kinase activation.
486 *J Biol Chem.* 2007;282(7):4516-23. doi: 10.1074/jbc.M605702200. PubMed
487 PMID: 17179149.
- 488 19. Lopez JM, Santidrian AF, Campas C, Gil J. 5-Aminoimidazole-4-carboxamide
489 riboside induces apoptosis in Jurkat cells, but the AMP-activated protein kinase is
490 not involved. *Biochem J.* 2003;370(Pt 3):1027-32. doi: 10.1042/BJ20021053.
491 PubMed PMID: 12452797; PubMed Central PMCID: PMCPMC1223217.
- 492 20. Xiang X, Saha AK, Wen R, Ruderman NB, Luo Z. AMP-activated protein kinase
493 activators can inhibit the growth of prostate cancer cells by multiple mechanisms.
494 *Biochem Biophys Res Commun.* 2004;321(1):161-7. doi:

- 495 10.1016/j.bbrc.2004.06.133. PubMed PMID: 15358229.
- 496 21. Guo F, Liu SQ, Gao XH, Zhang LY. AICAR induces AMPK-independent
497 programmed necrosis in prostate cancer cells. *Biochem Biophys Res Commun.*
498 2016. doi: 10.1016/j.bbrc.2016.04.077. PubMed PMID: 27103440.
- 499 22. Duan F, Li Y, Chen L, Zhou X, Chen J, Chen H, et al. Sulfur inhibits the growth
500 of androgen-independent prostate cancer in vivo. *Oncol Lett.* 2015;9(1):437-41.
501 doi: 10.3892/ol.2014.2700. PubMed PMID: 25436005; PubMed Central PMCID:
502 PMC4247018.
- 503 23. Boulares AH, Yakovlev AG, Ivanova V, Stoica BA, Wang G, Iyer S, et al. Role
504 of poly(ADP-ribose) polymerase (PARP) cleavage in apoptosis. Caspase
505 3-resistant PARP mutant increases rates of apoptosis in transfected cells. *J Biol*
506 *Chem.* 1999;274(33):22932-40. PubMed PMID: 10438458.
- 507 24. Barrett CS, Millena AC, Khan SA. TGF-beta Effects on Prostate Cancer Cell
508 Migration and Invasion Require FosB. *Prostate.* 2017;77(1):72-81. doi:
509 10.1002/pros.23250. PubMed PMID: 27604827; PubMed Central PMCID:
510 PMC5286811.
- 511 25. Petrylak DP, Tangen CM, Hussain MH, Lara PN, Jr., Jones JA, Taplin ME, et al.
512 Docetaxel and estramustine compared with mitoxantrone and prednisone for
513 advanced refractory prostate cancer. *N Engl J Med.* 2004;351(15):1513-20. doi:

- 514 10.1056/NEJMoa041318. PubMed PMID: 15470214.
- 515 26. Tannock IF, de Wit R, Berry WR, Horti J, Pluzanska A, Chi KN, et al. Docetaxel
516 plus prednisone or mitoxantrone plus prednisone for advanced prostate cancer. N
517 Engl J Med. 2004;351(15):1502-12. doi: 10.1056/NEJMoa040720. PubMed
518 PMID: 15470213.
- 519 27. Williams T, Courchet J, Viollet B, Brenman JE, Polleux F. AMP-activated
520 protein kinase (AMPK) activity is not required for neuronal development but
521 regulates axogenesis during metabolic stress. Proc Natl Acad Sci U S A.
522 2011;108(14):5849-54. doi: 10.1073/pnas.1013660108. PubMed PMID:
523 21436046; PubMed Central PMCID: PMC3078367.
- 524 28. Zhou W, Marcus AI, Vertino PM. Dysregulation of mTOR activity through
525 LKB1 inactivation. Chin J Cancer. 2013;32(8):427-33. doi:
526 10.5732/cjc.013.10086. PubMed PMID: 23668926; PubMed Central PMCID:
527 PMC3845579.
- 528 29. Khan AS, Frigo DE. A spatiotemporal hypothesis for the regulation, role, and
529 targeting of AMPK in prostate cancer. Nat Rev Urol. 2017;14(3):164-80. doi:
530 10.1038/nrurol.2016.272. PubMed PMID: 28169991; PubMed Central PMCID:
531 PMC3845579.
- 532 30. Hawley SA, Ross FA, Chevzoff C, Green KA, Evans A, Fogarty S, et al. Use of

- 533 cells expressing gamma subunit variants to identify diverse mechanisms of
534 AMPK activation. *Cell Metab.* 2010;11(6):554-65. doi:
535 10.1016/j.cmet.2010.04.001. PubMed PMID: 20519126; PubMed Central
536 PMCID: PMCPMC2935965.
- 537 31. Chen L, Han F, Qu H, Yan H, Ren L, Yang S. Combination therapy with
538 5-amino-4-imidazolecarboxamide riboside and arsenic trioxide in acute myeloid
539 leukemia cells involving AMPK/TSC2/mTOR pathway. *Pharmazie.*
540 2013;68(2):117-23. PubMed PMID: 23469683.
- 541 32. Santidrian AF, Gonzalez-Girones DM, Iglesias-Serret D, Coll-Mulet L, Cosialls
542 AM, de Frias M, et al. AICAR induces apoptosis independently of AMPK and
543 p53 through up-regulation of the BH3-only proteins BIM and NOXA in chronic
544 lymphocytic leukemia cells. *Blood.* 2010;116(16):3023-32. doi:
545 10.1182/blood-2010-05-283960. PubMed PMID: 20664053.
- 546 33. Su RY, Chao Y, Chen TY, Huang DY, Lin WW. 5-Aminoimidazole-4-
547 carboxamide riboside sensitizes TRAIL- and TNF{alpha}-induced cytotoxicity in
548 colon cancer cells through AMP-activated protein kinase signaling. *Mol Cancer*
549 *Ther.* 2007;6(5):1562-71. doi: 10.1158/1535-7163.MCT-06-0800. PubMed PMID:
550 17513605.
- 551 34. Bubendorf L, Schopfer A, Wagner U, Sauter G, Moch H, Willi N, et al.

552 Metastatic patterns of prostate cancer: an autopsy study of 1,589 patients. Hum

553 Pathol. 2000;31(5):578-83. PubMed PMID: 10836297.

554 35. Poorthuis MHF, Vernooij RWM, van Moorselaar RJA, de Reijke TM. First-line

555 non-cytotoxic therapy in chemotherapy-naive patients with metastatic

556 castration-resistant prostate cancer: a systematic review of 10 randomised clinical

557 trials. BJU Int. 2017;119(6):831-45. doi: 10.1111/bju.13764. PubMed PMID:

558 28063195.

559

560

561

562

563

564

565

566

567

568

569

570

571

572

573 **Figure legends**

574 Figure 1. The effect of AICAR on the growth of prostate cancer cells. (A) 22Rv1 cells
575 were treated with different concentration of AICAR for 24 hr. The cell viability was
576 measured by the MTT assay. (B) 22Rv1 cells were treated with different
577 concentration of AICAR, and then grown in soft agar, an anchorage-independent
578 condition, for 3 weeks. Colonies were stained with crystal violet and captured using
579 Bio-Rad ChemiDoc XRS⁺ system. Data are represented as means \pm SD of triplicate
580 values and statistical significance was determined using the Student's *t*-test (***p*<
581 0.01; ****p*< 0.001).

582

583 Figure 2. Effect of AICAR on the apoptosis in 22Rv1 prostate cancer cells. Cells were
584 incubated with different concentrations of AICAR for 24 hr. (A) Cells were collected,
585 stained with Annexin V and PI, and analyzed by flow cytometry. Data are
586 representative of at least three independent experiments with similar results. (B) The
587 expression of PARP was determined by Western blot. Actin was used as a loading
588 control in Western blot. (C) Cellular caspase 3/7 activities were analyzed with
589 caspase-glo assay kit. Data are represented as means \pm SD of triplicate values and

590 statistical significance was determined using the Student's *t*-test ($***p < 0.001$).

591

592 Figure 3. Effect of AICAR on the cell migration activity in 22Rv1 prostate cancer

593 cells. Cells were seeded in SPLScar™ Block overnight, the block was then removed

594 and cells were treated with 5 ng/ml TGF-β1 and different concentrations of AICAR.

595 (A) Cell migration was monitored under a phase-contrast microscope. Data are

596 representative of at least three independent experiments with similar results. (B) The

597 migratory distance was calculated. Data are represented as means ± SD of triplicate

598 values and statistical significance was determined using the Student's *t*-test ($*p < 0.05$;

599 $**p < 0.01$; $***p < 0.001$). (C) The expression of N-cadherin and E-cadherin was

600 analyzed by Western blot. Actin was used as a loading control in Western blot. The

601 Western blotting results are representative of results obtained in three separate

602 experiments.

603

604 Figure 4. Effect of AICAR on the sensitivity of 22Rv1 prostate cancer cells to

605 docetaxel treatment. Cells were treated with different concentrations of AICAR in the

606 presence or absence of docetaxel for 24 hr. The cell viability was measured by the

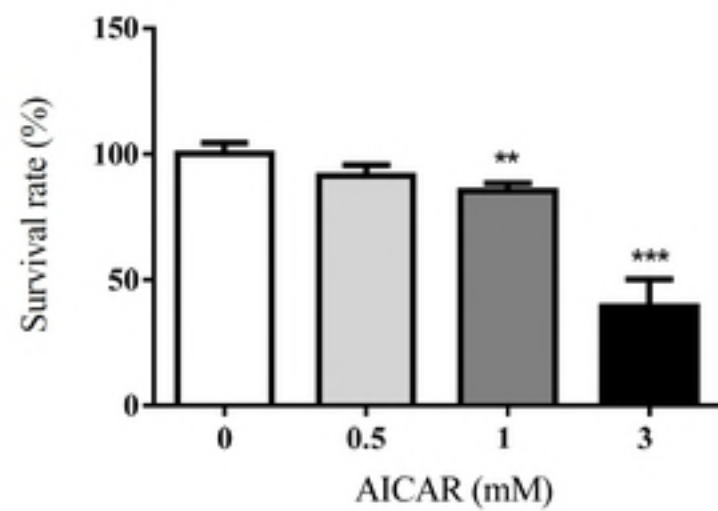
607 MTT assay. Data are represented as means ± SD of triplicate values and statistical

608 significance was determined using the Student's *t*-test ($*p < 0.05$; $**p < 0.01$).

609

610 Figure 5. Effect of AICAR on the AMPK/mTOR-dependent pathway in 22Rv1
611 prostate cancer cells. Cells were treated with different concentrations of AICAR for 2
612 hr. The expression of (A) phospho-AMPK, AMPK, (B) TSC1 and TSC2 was
613 examined by Western blot. Cells were treated with different concentrations of AICAR
614 for 6 hr. (C) The expression of mTOR, cMYC, phosphor-p70S6K and p70S6K was
615 determined by Western blot. Actin was used as a loading control in Western blot. The
616 Western blotting results are representative of results obtained in three separate
617 experiments. (D) Proposed mechanism of the anticancer effects induced by AICAR in
618 22Rv1 prostate cancer cells.

A



B

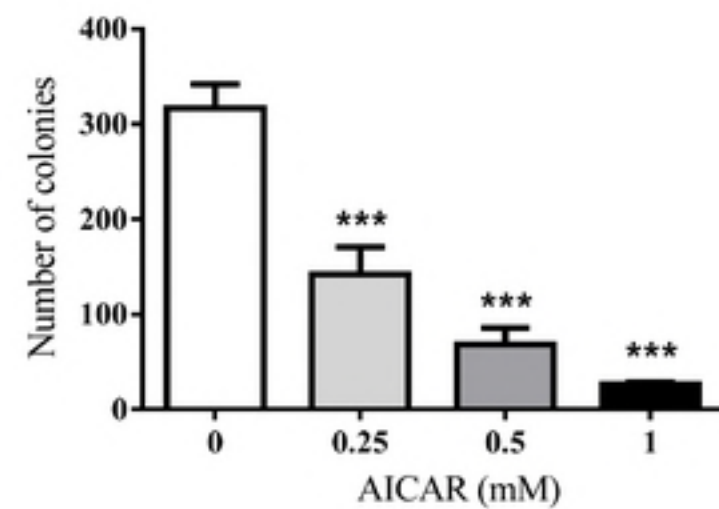
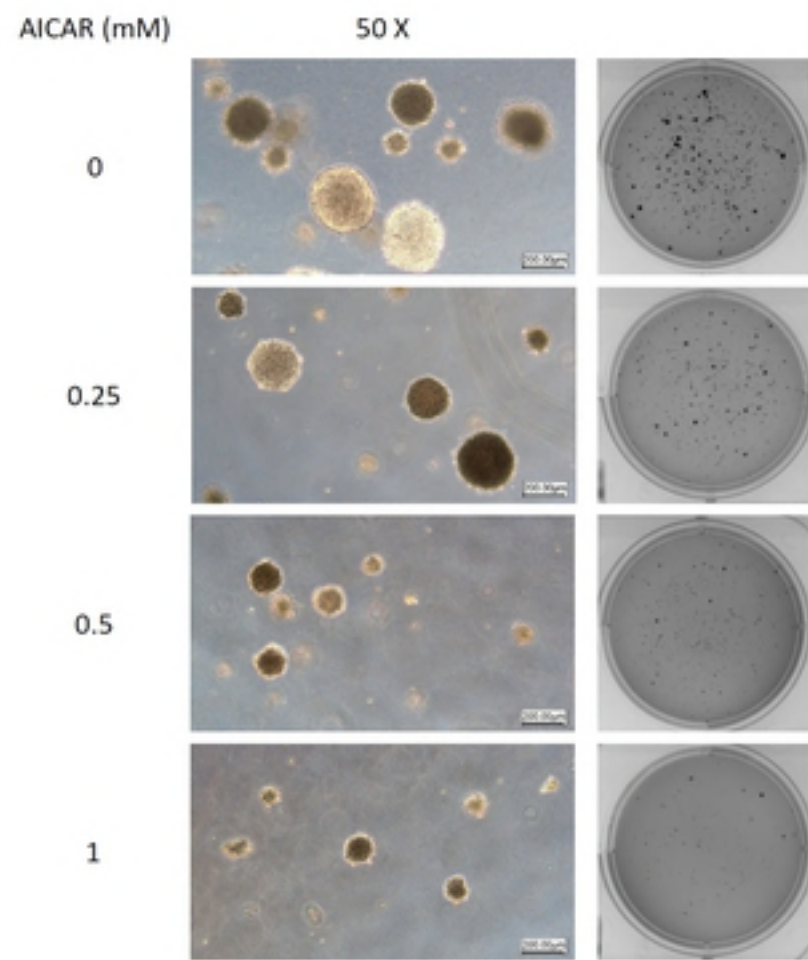
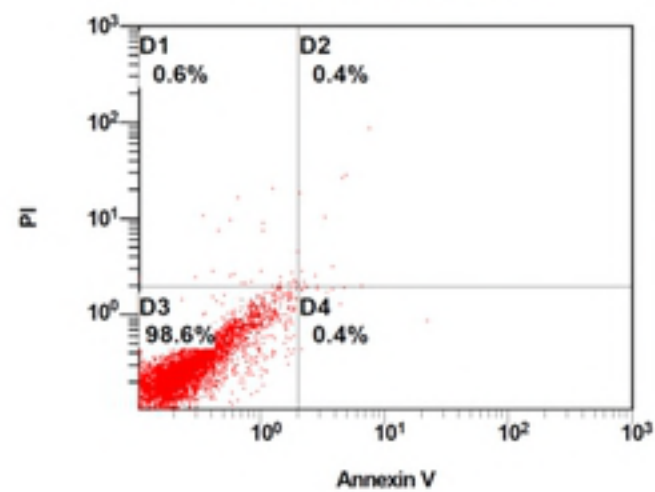


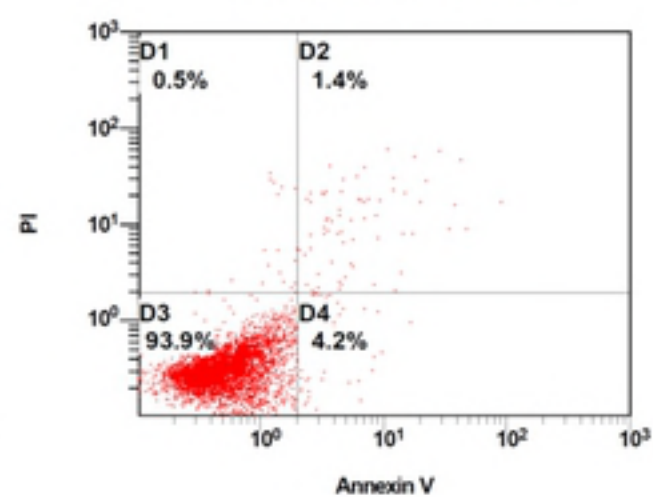
Figure 1

A

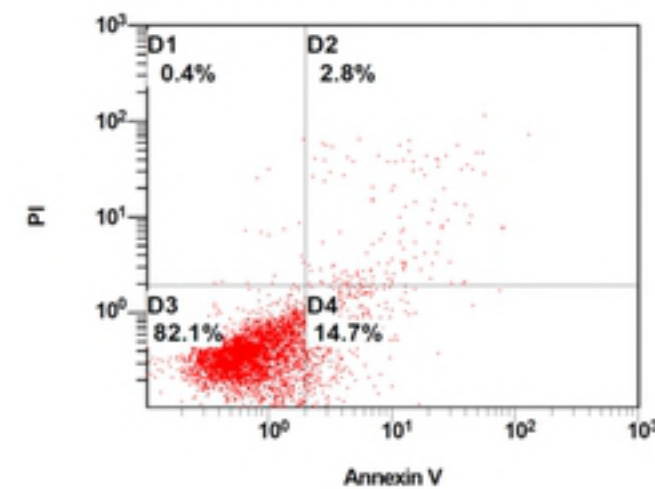
AICAR 0 mM



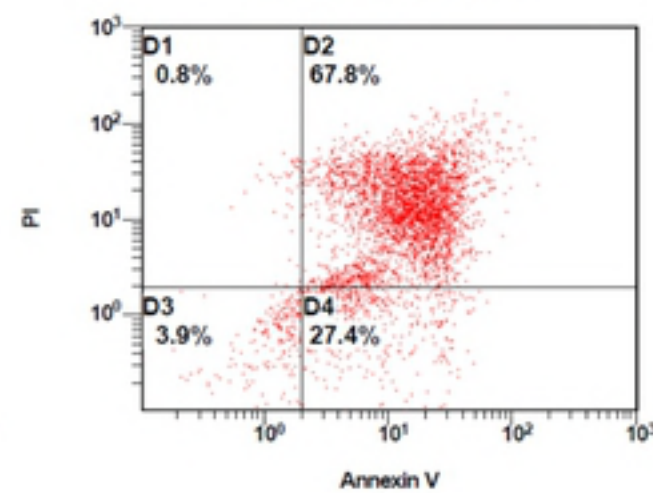
AICAR 0.5 mM



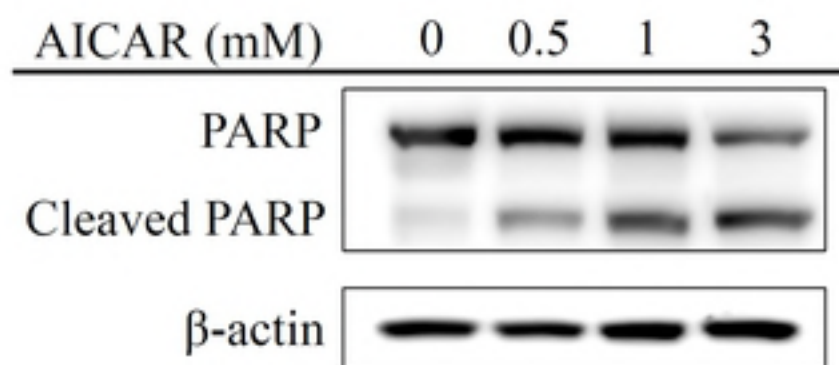
AICAR 1 mM



AICAR 3 mM



B



C

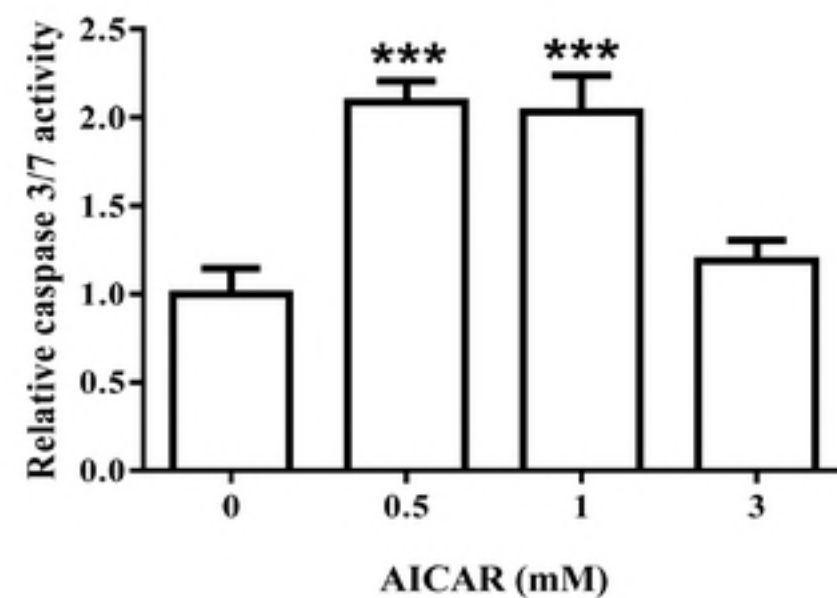
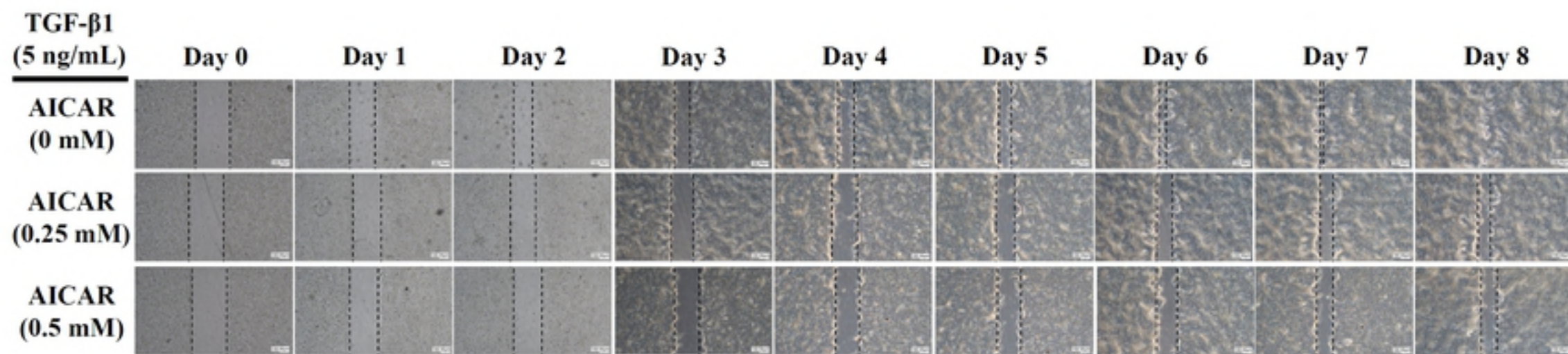
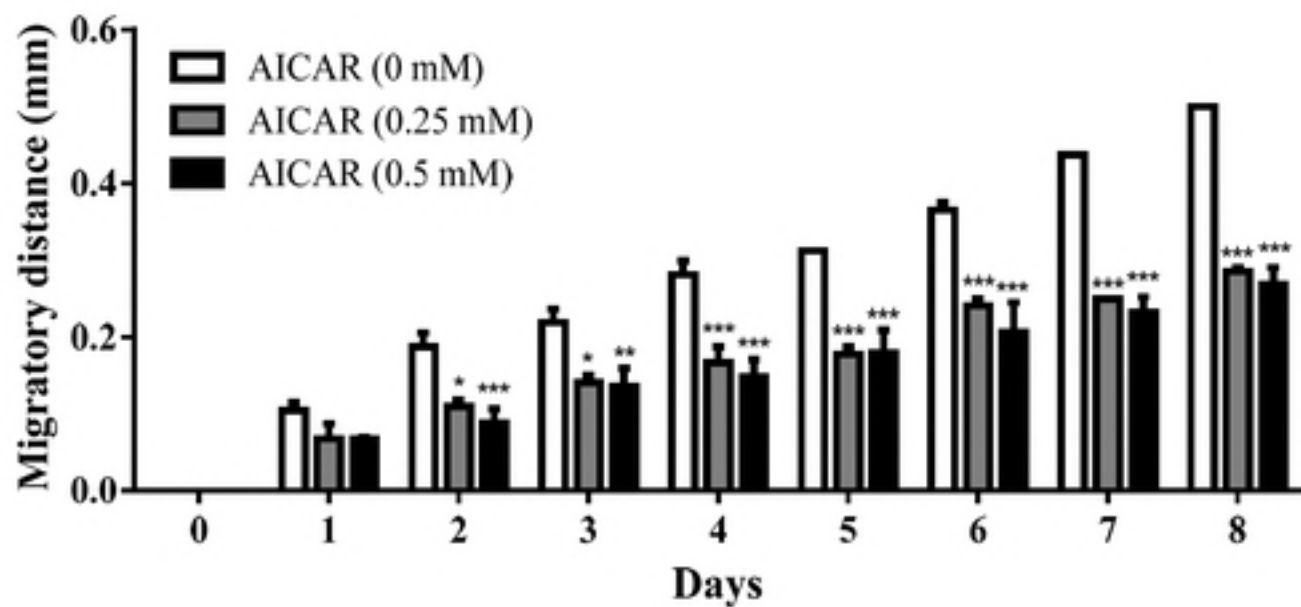


Figure 2

A



B



C

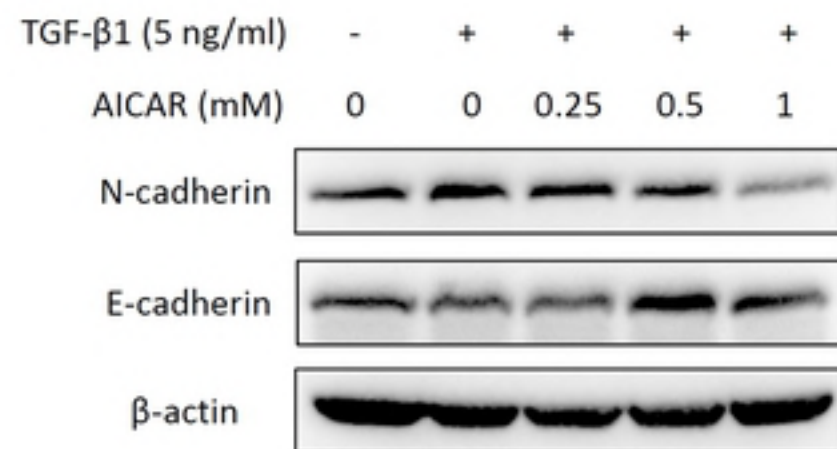


Figure 3

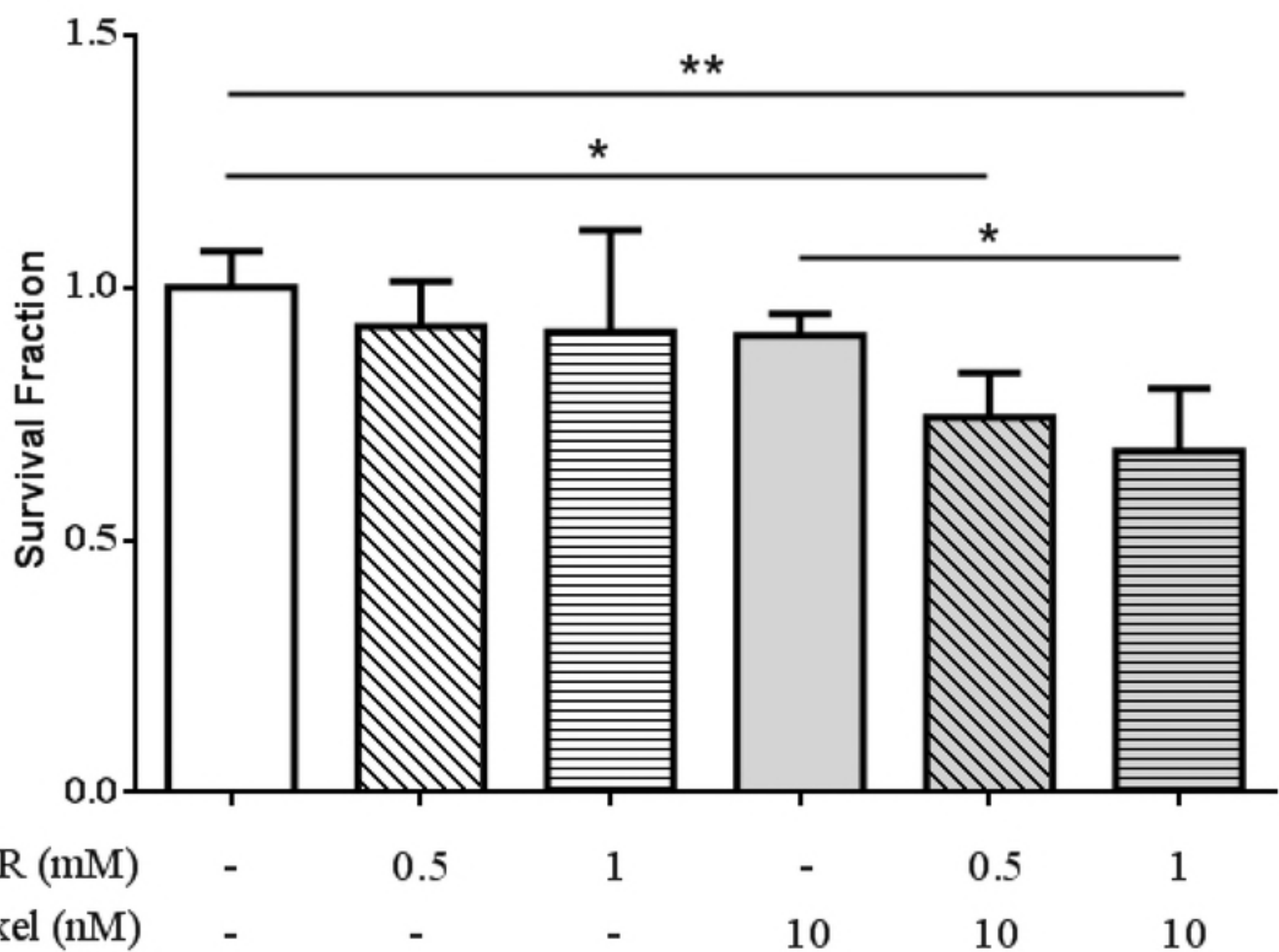
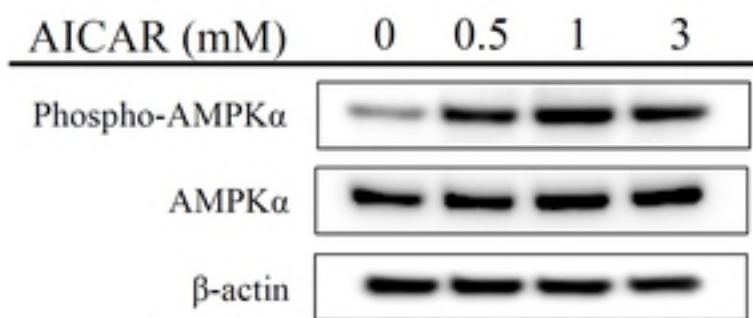
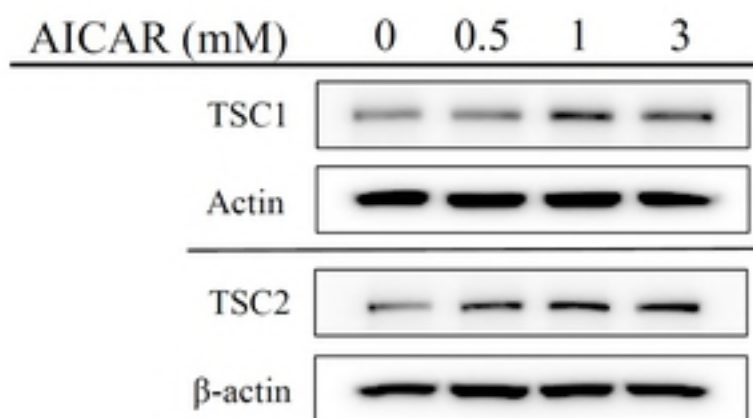


Figure 4

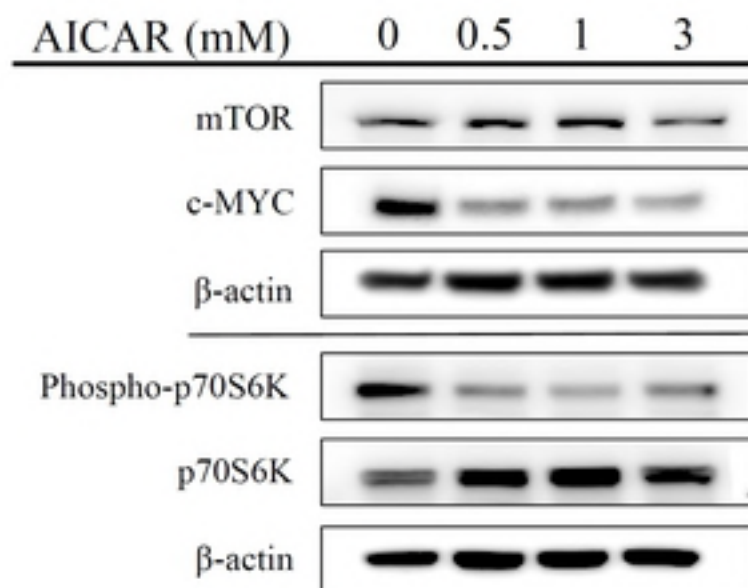
A



B



C



D

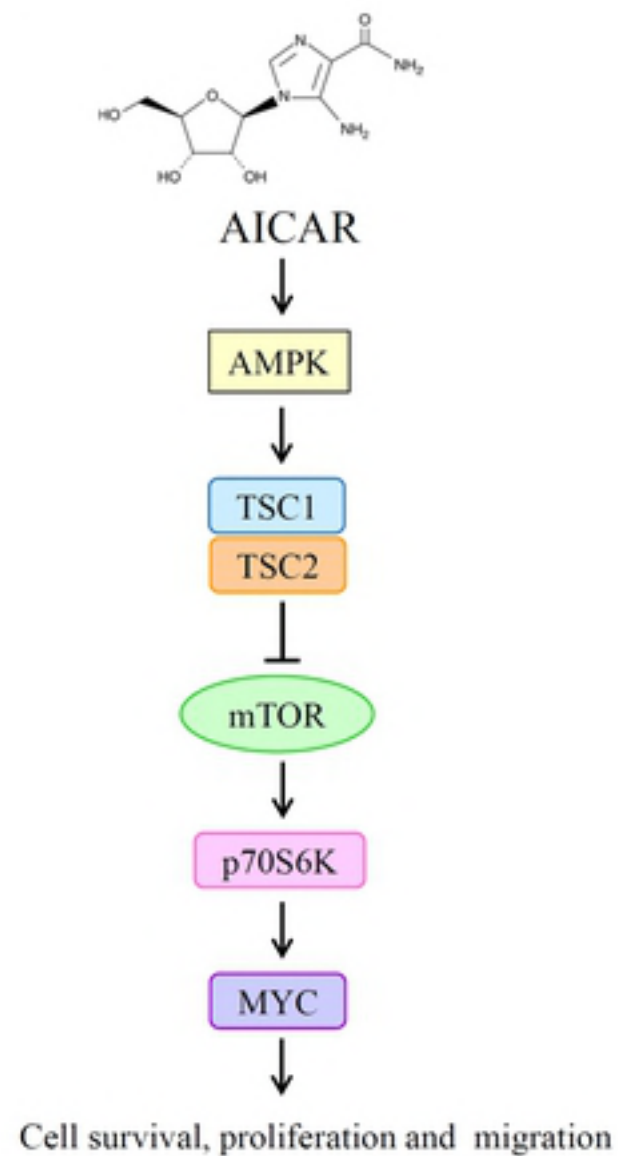


Figure 5